

# Atomic Layer Deposition and Characterization of Stoichiometric Erbium Oxide Thin Films on Si(100) using (CpMe)<sub>3</sub>Er Precursor and Ozone

Runshen Xu,<sup>a</sup> Qian Tao,<sup>a</sup> Yi Yang,<sup>a</sup> and Christos G. Takoudis<sup>a,b</sup>

<sup>a</sup> *Department of Chemical Engineering, University of Illinois at Chicago, Chicago, Illinois 60607*

<sup>b</sup> *Department of Bioengineering, University of Illinois at Chicago, Chicago, Illinois 60607*

## Abstract

Thin stoichiometric erbium oxide films were atomic layer deposited on p-type Si(100) substrates using tris(methylcyclopentadienyl)erbium and ozone. The film growth rate was found to be  $0.12 \pm 0.01$  nm/cycle with an atomic layer deposition temperature window of 170-330 °C. X-ray photoelectron spectral (XPS) analysis of the resulting Er<sub>2</sub>O<sub>3</sub> films indicated the as-deposited films to be stoichiometric with no evidence of carbon contamination. Studies of post deposition annealing effects on resulting films and interfaces were done using Fourier transforms infrared spectroscopy, XPS, glancing incidence X-ray diffraction, and optical surface profilometry. As-deposited Er<sub>2</sub>O<sub>3</sub> films were found to crystallize in the cubic structure with dominant (222) orientation; no erbium silicate was found at the interface. After annealing at 800 °C in N<sub>2</sub> for 5 min, a new XPS feature was found and it was assigned to the formation of erbium silicate. As the annealing temperature was increased, the interfacial erbium silicate content was found to increase in the temperature range studied.

## 1. Introduction

Structural and interfacial studies of high dielectric constant ( $\kappa$ ) materials are important in the continuous scaling of nanoelectronics such as complementary metal oxide semiconductors and dynamic random-access memories (DRAM).[1] The use of traditional  $\text{SiO}_2$  as a gate dielectric layer less than 1.5 nm-thick has reached its fundamental limit because of the excess direct tunneling leakage current. So far, various lanthanide oxides, such as  $\text{Gd}_2\text{O}_3$ ,  $\text{Pr}_2\text{O}_3$ , and  $\text{Er}_2\text{O}_3$ , have been considered as possible alternative gate dielectrics.[2-8] From these oxides,  $\text{Er}_2\text{O}_3$  attracts increasing attention in terms of its large conduction band offset to Si (3.5 eV), moderately high dielectric constant (i.e., 14 -17) and good thermal stability with silicon.[2, 9-11] In addition, when compared with other lanthanide elements, erbium has appropriate electronegativity and small ionic radius, which result in limited tendency to hydroxylation.[12]

$\text{Er}_2\text{O}_3$  has been grown with various deposition techniques, such as RF sputtering,[13] electron beam evaporation,[14] metal-organic chemical vapor deposition (MOCVD),[15, 16] and atomic layer deposition (ALD).[7, 17, 18] Among these techniques, ALD has been identified as a preferred technique for high-k applications in order to maintain precise thickness at the needed dimensions within metal oxide semiconductor field effect transistors and to provide conformal coverage along the deep trenches of DRAM cells.[1] In early ALD studies of  $\text{Er}_2\text{O}_3$ , the precursor used was mainly tris(2,2,6,6, tetramethyl-3,5 heptanedione) erbium,  $\text{Er}(\text{thd})_3$ . For example, Paivasaari et al. used  $\text{Er}(\text{thd})_3$  with ozone as the oxidant and found the deposition process to have a low growth rate ( $\sim 0.025$  nm/cycle) at temperatures between 250 and 375 °C.[17] The resulting erbium oxide thin films were reported to be oxygen-rich ( $\text{O}/\text{Er} = 1.7$ ) with

carbon, hydrogen and fluorine contents of 1.8, 4 and 1.7 %, respectively. A higher growth rate and reduced impurities were demonstrated by using tris(amidinate) precursors,  $\text{Er}(\text{}^t\text{Bu}_2\text{amd})_3$ , and ozone,[7] i.e.,  $\sim 0.05$  nm/cycle at 270 °C. However, the growth rate was reported to increase with precursor pulse duration, which was likely due to partial thermal decomposition of  $\text{Er}(\text{}^t\text{Bu}_2\text{amd})_3$  during the precursor delivery process; the stoichiometric ratio O/Er of those films was found to be 1.8 with a carbon content of 1.8 %. In both studies of  $\beta$ -diketonate and amidinate types of erbium precursors, as-deposited  $\text{Er}_2\text{O}_3$  was found to be amorphous at deposition temperatures below 250 °C, but started to crystalize into a polycrystalline cubic structure at a temperature of 250 - 350 °C. Recently, cyclopentadienyl precursors were used to deposit other metal oxide films.[19-21] When compared with  $\beta$ -diketonate and amidinate ligands precursors, cyclopentadienyl-type precursors exhibit good thermodynamic stability. In addition, cyclopentadienyl compounds have a relatively low sublimation temperature which leads to a high ALD growth rate due to its moderate vapor pressure.[6, 22]

Tris(methylcyclopentadienyl)erbium,  $(\text{CpMe})_3\text{Er}$ , was used with water vapor to deposit  $\text{Er}_2\text{O}_3$  thin films on silicon.[18] The deposition rate was reported to be  $\sim 0.15$  nm/cycle at 250 - 350 °C; the resulting films were found to be overstoichiometric (O/Er = 1.7) with a carbon content of  $\sim 2.5$  %. The oxygen-rich O/Er composition was attributed to hydroxylation reaction between erbium oxide and water vapor.

In this study, the cyclopentadienyl ligand erbium precursor tris(methylcyclopentadienyl) erbium is used with ozone as the oxidant to deposit  $\text{Er}_2\text{O}_3$  thin films on silicon (100) by ALD. A wide ALD window as well as a growth rate of 0.12 nm/cycle are found. Elemental quantitative analysis of as-deposited  $\text{Er}_2\text{O}_3$  films indicates that the films are *stoichiometric* (O/Er=1.5) with *no*

evidence of detectable carbon contamination. Post deposition annealing temperatures of 600-1000°C are used for studies on the annealing behavior of the resulting ALD films; after annealing, changes in  $\text{Er}_2\text{O}_3$  film structure, interfacial layer, and surface morphology are presented and discussed using a variety of analytical techniques.

## **2. Experimental**

Erbium oxide thin films were deposited using tris(methylcyclopentadienyl)erbium precursor and ozone as oxidant on Si(100) substrates in a horizontal hot wall tubular ALD reactor using a quartz tube 38 mm in diameter and 48 cm in length (Fig. 1). The reactor can be operated at a temperature up to 600 °C (custom-modified processing furnace, model 1043 Marshall, ThermCraft, Inc.) and typical depositions can be carried out at the temperature range of 25 - 450 °C. The base pressure of the ALD reactor was less than 20 mTorr. The oxidant was mixture of ozone and oxygen (1000 ppm ozone) generated with an oxygen (99.999% purity) flow through a UV lamp ozone generator immediately upstream of the deposition reactor. Argon (99.999% purity) was used as both carrier gas for the metal precursor and purging gas to clean the system between the delivery of precursor and oxidant. The precursor bubbler was kept at 95 °C, and the delivery line section from the bubbler to the reactor was maintained 20-30 °C higher than the bubbler temperature in order to prevent condensation of the precursor during delivery. The depositions of  $\text{Er}_2\text{O}_3$  films were carried out at a total pressure of 500 mTorr and in the temperature range of 100-400 °C.

Er<sub>2</sub>O<sub>3</sub> films were deposited on p-type Si (100) substrates (15 mm × 20 mm). Prior to deposition, substrates were cleaned with a 1:1:5 NH<sub>4</sub>OH:H<sub>2</sub>O<sub>2</sub>:H<sub>2</sub>O solution for 15 min to remove organic contaminants and particles, followed by 1% HF dip for 10 s. Each of the steps was followed by thorough deionized (DI) water rinse and drying by N<sub>2</sub> gas. This cleaning was found to leave ~ 0.5 nm (as measured by ellipsometry) of native oxide on the silicon substrate surface.

Thicknesses of as-deposited films were measured with a spectral ellipsometer (J.A. Woollam Co., Inc., model M44). Post deposition annealings were carried out in a preheated quartz horizontal furnace (Lindberg Blue three-zone furnace) under N<sub>2</sub> atmosphere for 5 min between 600 and 1000 °C at 1 atm. Fourier transforms infrared (FTIR) spectroscopy (Nicolet, Magna-IR 560) was used in the transmission mode over the wavelength range of 4000-400 cm<sup>-1</sup>. A high resolution X-ray diffractometer (Philips X'pert) configured with 0.1542 nm X-ray emission line of Cu with bandwidth of 0.05 nm as the excitation source was used to obtain glancing incidence X-ray diffraction (GIXRD) diffractograms of ~ 30 nm-thick as-deposited and post annealed Er<sub>2</sub>O<sub>3</sub> films at 600, 800 and 1000 °C in N<sub>2</sub> (99.999% purity) at 1 atm. GIXRD diffractograms were collected at an incident angle of 0.7° to enhance the diffraction sensitivity within the film and to avoid interference from the single crystal Si(100) substrate. The peaks were identified using the International Centre for Diffraction Data (ICDD) database of diffraction pattern Powder Diffraction Files (PDF). Chemical bonding and elemental analyses of Er<sub>2</sub>O<sub>3</sub> films were probed with high resolution X-ray Photoelectron Spectroscopy (XPS) (Kratos Analytical Ltd., Kratos AXIS-165) equipped with a monochromatic Al K $\alpha$  (1486.6 eV) X-ray source operating at 15 kV and 10 mA. High resolution spectra were collected at a take-off angle 90° with pass energy of 20 eV, step size of 0.1 eV, and dwell time of 200 ms. Surface morphology of as-deposited and post

annealed thin films was studied using an optical surface profiler system (Veeco Instrument Inc., model Wyko NT3300) in the phase-shifting interferometry (PSI) mode with a vertical resolution of 0.1 nm.

### 3. Results and Discussion

#### 3.1 ALD temperature window and growth rate of $\text{Er}_2\text{O}_3$ thin films

The thin film growth rate dependence on reactor temperature is shown in Figure 2. The error bar value shows less than 3% of thickness variation across the whole deposition area. At the lower deposition temperature region of 100-170 °C, a higher deposition rate that decreased with increasing substrate temperature was observed indicating a nonself-limiting film growth behavior because of likely precursor condensation on the substrate. Compared with other ALD  $\text{Er}_2\text{O}_3$  studies that utilized different precursors, [7, 17-18] a wider ALD temperature window in the range of 170-330 °C was observed, with a growth rate of  $0.12 \pm 0.01$  nm/cycle. A decrease in the deposition rate is found at substrate temperatures higher than 330 °C, and that is likely due to lower adsorption of  $(\text{CpMe})_3\text{Er}$  on the surface. Figure 3 shows the thickness of the as-deposited  $\text{Er}_2\text{O}_3$  films measured after different number of cycles, i.e., from 15 to 300. From the slope of linear regression analysis of the data, the growth rate is found to be  $\sim 0.12$  nm/cycle. In this case, the growth rate of  $\text{Er}_2\text{O}_3$  is lower than that reported using  $(\text{CpMe})_3\text{Er}/\text{H}_2\text{O}$ , [18] but much higher than that from other studies with different Er precursors, such as  $\text{Er}(\text{thd})_3$  or  $\text{Er}(\text{t}^{\text{Bu}}_2\text{amd})_3$  and ozone or oxygen plasma as the oxidant.[7, 17, 23] The self-limiting nature of ALD is also represented by the high degree of uniformity of the film thickness.

### 3.2 Fourier transform infrared spectroscopy studies

Figure 4 shows the FTIR transmission spectra of 15 nm-thick  $\text{Er}_2\text{O}_3$  films as-deposited and subsequently annealed in  $\text{N}_2$  at 600, 800, and 1000 °C for 5 min. Spectra were collected with 90° take-off angle. The IR spectra of the resulting films were obtained by subtracting the substrate reference spectrum obtained from the Si(100) substrate after the cleaning process. As seen in Fig. 4, the spectrum of the as-deposited film shows small peaks at 440 and 600  $\text{cm}^{-1}$  that can be assigned to phonon bands of crystallized  $\text{Er}_2\text{O}_3$  cubic phase.[13, 24] This suggests the onset of film crystallization under such deposition conditions, i.e., at 250 °C. For the films annealed at 600 °C, the appearance of sharper peaks at those low wave numbers (440 and 600  $\text{cm}^{-1}$ ) suggests more intense phonon bands of the cubic phase crystal structure of  $\text{Er}_2\text{O}_3$ . The intensity of the features in this region (400-650  $\text{cm}^{-1}$ ) increases with higher annealing temperature up to 1000 °C, which is attributed to the increasing crystallinity of  $\text{Er}_2\text{O}_3$  films. In the wave length region of 800-1000  $\text{cm}^{-1}$ , a weak feature is observed (at  $\sim 900 \text{ cm}^{-1}$ ) for the film annealed at 1000 °C and this seems to be consistent with that reported by Ono et al,[4] who attributed it to IR absorption of Si-O-Er bonds forming at a high annealing temperature. The absence of peaks in the 1300-3200  $\text{cm}^{-1}$  region suggests that the carbon content in the films is below detectable level, which is corroborated by independent XPS studies (see later sections).

### 3.3 Chemical shifts and compositional analyses by XPS

#### 3.3.1 XPS spectra of as-deposited films

Figure 5 shows high resolution XPS spectra of an as-deposited  $\text{Er}_2\text{O}_3$  2 nm-thick film on silicon. It includes the core level spectra of Er 4d, O 1s, and Si 2p. The Er 4d spectrum (inset of Fig. 5a) was fitted with one Gaussian-Lorentzian distribution at 168.8 eV corresponding to  $\text{Er}^{3+}$ ; this

indicates that the film is composed of  $\text{Er}_2\text{O}_3$  without formation of non-stoichiometric erbium oxide.[25, 26] The higher binding energy peak resulting from the chemical state of  $\text{SiO}_2$  cannot be observed because of the overlap of the  $\text{Si}^{4+}$  and  $\text{Er}^{3+}$  auger peaks. The O 1s spectrum (Figure 5b) could be deconvoluted into two symmetric peaks attributed to different chemical bonding states of the  $\text{Er}_2\text{O}_3/\text{Si}$  system. The low energy state centered at 529.7 eV is attributed to oxygen in  $\text{Er}_2\text{O}_3$ . The higher bonding energy state, at 532.2 eV, is assigned to Si-O bonds.[25] This also indicated that the interfacial layer consisted of silicon dioxide without formation of erbium silicate during the ALD.

Figure 6 shows the C 1s spectra of 30 nm-thick  $\text{Er}_2\text{O}_3$  films deposited on Si substrates. The spectra were collected before and after etching the film with  $\text{Ar}^+$  beam in order to differentiate carbon on the surface from that in the bulk film. Before the removal of surface contaminants, the elemental ratios of O:Er:C are quantitatively determined to be 57.5:38.3:4.2 atom %. The ratio of O/Er corresponds to stoichiometric  $\text{Er}_2\text{O}_3$ , in contrast to the earlier ALD studies with different precursors.[7,17, 18] After sputtering the surface using  $\sim 300$  nA of  $\text{Ar}^+$  beam for 10 min, the amount of carbon is below detectable level, i.e., less than 0.5 atom %. Losurdo et al. reported that their MOCVD  $\text{Er}_2\text{O}_3$  films resulting from  $\text{Er}(\text{Cp}^i\text{Pr})_3$  and  $\text{O}_2$  were close to the stoichiometric ratio.[16] However, studies on  $\text{Er}_2\text{O}_3$  thin films deposited by e-beam evaporation and ALD were oxygen-rich (O/Er = 1.6-1.8) with carbon incorporation.[7, 17, 18, 27] This was likely due to the formation of  $\text{Er}(\text{OH})_3$  and  $\text{Er}_2\text{O}_2\text{CO}_3$ , the probable result of interactions between  $\text{Er}_2\text{O}_3$  and moisture or carbon oxide.[7, 13, 27]



### 3.3.2 XPS analyses of annealed films

Figure 7 (a) shows the changes in the core level of Er 4d spectra for 3 nm-thick  $\text{Er}_2\text{O}_3$  films post deposition annealed in  $\text{N}_2$  at 600, 800 and 1000 °C. The Er 4d peak is found to up shift as the annealing temperature increases from 600 to 1000 °C. The Er 4d spectrum of  $\text{Er}_2\text{O}_3$  films annealed at 600 °C was similar to that of the as-deposited film (e.g., inset of Fig.5 (a)) and it could not be deconvoluted into more than one Gaussian-Lorentzian subordinate peak at 168.8 eV.[26] This suggests that films annealed at 600 °C consisted of unchanged  $\text{Er}_2\text{O}_3$ . For the film annealed at 800 °C, the higher binding energy peak upon deconvolution resulted in an additional feature at 169.6 eV, which is attributed to the formation of  $\text{ErSiO}_x$ . Further, the spectrum of the sample annealed at 1000 °C showed increased intensity of the 169.6 eV peak, indicative of increased silicate formation; this is likely because the interdiffusion between the  $\text{Er}_2\text{O}_3$  film and the interfacial  $\text{SiO}_2$  during this annealing process.

Figure 7 (b) illustrates the core level O 1s XPS spectra for the same annealed 3 nm-thick  $\text{Er}_2\text{O}_3$  films. O 1s spectra of the annealed films at 600 °C shows two peaks at 529.7 and 532.2 eV, assigned to  $\text{Er}_2\text{O}_3$  (529.7 eV) and  $\text{SiO}_2$  (532.2 eV). O 1s spectra of films annealed at 800 and 1000 °C could be deconvoluted into three Gaussian-Lorentzian subordinate peaks centered at 529.9 eV (Er-O), 531.4 eV (Er-O-Si) and 532.3 eV (Si-O), respectively, which are in agreement with the assignments of erbium oxide and silicate presented in Fig 7 (a) and discussed. At 1000 °C, the intensity of the peaks at 529.9 eV and 532.3 eV decreases while the feature at 531.4 eV is seen to increase. The erbium silicate content is indeed found to increase during annealing from 800 to 1000 °C, and the silicate peak becomes the dominant one; also, the O 1s spectral component assigned to Si-O down shifts from 532.2 to 531.9 eV, which also corroborates the

increasing presence of erbium silicate. Increased silicate formation at 800 °C is consistent with an earlier XPS study of films deposited by physical evaporation.[28] However, Losurdo et al. reported that the onset temperature of formation of erbium silicate was 600 °C.[16]

### 3.4 GIXRD studies of Er<sub>2</sub>O<sub>3</sub> thin films

Figure 8 shows the GIXRD spectra of as-deposited Er<sub>2</sub>O<sub>3</sub> films as well as films post deposition annealed at 600, 800 and 1000 °C in N<sub>2</sub> for 5 min; the thickness of all films is 30 nm. The peak at 29.7 ° for the as-deposited films indicates the onset of film crystallization under the ALD conditions used, i. e., 250 °C. Upon annealing, another two weak diffraction peaks at 34.2 ° and 49.1 ° are observed when the annealing temperature is 800 °C or higher. The intensity of these cubic crystalline peaks increased with higher post-deposition annealing temperatures (up to 1000 °C), suggesting increased crystallinity of the Er<sub>2</sub>O<sub>3</sub> films with higher annealing temperature conditions. The major peaks have been identified to be in the cubic phase with the (222) orientation dominance (ICDD cards: 008-8242 and 26-0604).[18] The average lattice constant (calibrated by Jade 9.0 software calculation of fitted peaks) is found to be about 1.047 nm for ALD Er<sub>2</sub>O<sub>3</sub> films (as-deposited and annealed at temperatures between 600 and 1000 °C) which is smaller than that of bulk Er<sub>2</sub>O<sub>3</sub> (a=1.055 nm). The grain sizes of the as-deposited and annealed films at 600, 800, and 1000 °C are 7.5, 8.2, 10.6 and 14.2 nm respectively, calculated by applying Scherrer's relation to the XRD (222), (400) and (440) peaks. In contrast, amorphous structure was found in earlier XRD studies of Er<sub>2</sub>O<sub>3</sub> films deposited from different ALD precursors. For example, as-deposited Er<sub>2</sub>O<sub>3</sub> films grown from Er(thd)<sub>3</sub> precursor at a temperature below 250 °C were reported to be amorphous with no observed diffraction peaks.[17]

Paivasaari et al. reported that as-deposited  $\text{Er}_2\text{O}_3$  films grown from  $\text{Er}(\text{}^t\text{Bu}_2\text{amd})_3$  precursor were also amorphous below 300 °C.[7]

### 3.5 Mapping of $\text{Er}_2\text{O}_3$ thin films using optical profilometry

The annealing effect on the surface morphology of 30 nm-thick  $\text{Er}_2\text{O}_3$  films studied using the PSI mode of an optical surface profiler (i.e., noncontact surface profilometry based on the interference of light to produce high-precision images of the surface) is shown in Figure 9.

As-deposited  $\text{Er}_2\text{O}_3$  films have a smooth surface and a root-mean-square (RMS) roughness of 0.71 nm (Figure 9(a)). The RMS roughness values of films annealed at 600, 800 and 1000 °C are found to be 0.75, 0.85 and 0.91 nm, respectively. The surface morphology and roughness is therefore found to barely increase from as-deposited to post annealed films in contrast with data reported in earlier related studies;[7, 17] this is likely because in those studies, post annealing could induce film crystallization from the amorphous structure of as-deposited films, while in our study, post annealing was found to enhance the crystallinity of as-deposited films that already had some crystallinity. It therefore indicates that the surface morphology/roughness can be more sensitive to phase transformations than to the enhancement of film crystallinity.

## 4. Conclusion

Ultrathin  $\text{Er}_2\text{O}_3$  films were deposited on p-type Si(100) substrates by atomic layer deposition using tris(methylcyclopentadienyl)erbium and ozone. The ALD temperature window for this process was found to be 170-330 °C. The growth rate of  $\text{Er}_2\text{O}_3$  with temperature-optimized ALD conditions was 0.12 nm/cycle. Elemental quantitative analysis of as-deposited  $\text{Er}_2\text{O}_3$  films

indicated the films were stoichiometric (O/Er=1.5) with no evidence of detectable carbon contamination. Upon annealing in N<sub>2</sub> for 5 min, XPS results suggested that the formation of erbium silicate was initiated at an annealing temperature greater than 600 °C and it was found to increase with increasing annealing temperature up to 1000 °C. FTIR analyses of Er<sub>2</sub>O<sub>3</sub> films annealed at 600 °C revealed sharper features corresponding to the cubic phase of Er<sub>2</sub>O<sub>3</sub>, and the intensity of the peaks increased with higher annealing temperature; this suggests increased film crystallinity with higher annealing temperatures in agreement with GIXRD results. The onset of film crystallization appeared in as-deposited films at the deposition temperature of 250 °C with an average lattice constant of 1.047 nm. In addition, both as-deposited and annealed films exhibited smooth surfaces with RMS values less than 1 nm; surface morphology of Er<sub>2</sub>O<sub>3</sub> films was found to become slightly rougher at post deposition annealing temperatures up to 1000 °C.

### **Acknowledgement**

The erbium precursor was provided to us by Dr. Christian Dussarrat (Air Liquid Group). This project was supported by the National Science Foundation (GOALI 0329195, CMMI 0609377 and EEC 0755115). We are also grateful to Dr. M. Sardela from the Frederick Seitz Materials Research Laboratory Central Facilities, University of Illinois for his expertise and input on our GIXRD studies.

## References

- [1] S. Guha, V. Narayanan, *Annu. Rev. Mater. Res* 39 (2009) 181.
- [2] K.B. Jinesh, Y. Lamy, E. Tios, W.F.A. Besling, *Appl. Phys. Lett.* 94 (2009) 252906.
- [3] J.M.J. Lopes, M. Roeckerath, T. Heeg, U. Littmark, J. Schubert, S. Mantl, Y. Jia, D.G. Schlom, *Microelectronic Engineering* 84 (2007) 1890.
- [4] H. Ono, T. Katsumata, *Appl. Phys. Lett.* 78 (2001) 1832.
- [5] K. Kakushima, K. Tsutsui, S.-I. Ohmi, P. Ahmet, V.R. Rao, H. Iwai, *Topics in Applied Physics* 106 (2007) 345.
- [6] J. Paivasaari, J. Niinisto, P. Myllymaki, C. Dezelah, C.H. Winter, M. Putkonen, M. Nieminen, L. Niinisto, *Topics in Applied Physics* 106 (2007) 15.
- [7] J. Paivasaari, C.L. Dezelah, D. Back, H.M. El-Kadri, M.J. Heeg, M. Putkonen, L. Niinisto, C.H. Winter, *J. Mater. Chem.* 15 (2005) 4224.
- [8] J. Paivasaari, M. Putkonen, L. Niinisto, *Thin Solid Films* 472 (2005) 275.
- [9] M. Losurdo, M.M. Giangregorio, G. Bruno, D. Yang, E.A. Irene, A.A. Suvorova, M. Saunders, *Appl. Phys. Lett.* 91 (2007) 091914.
- [10] C. Adelhelm, T. Pickert, M. Balden, M. Rasinski, T. Plocinski, C. Ziebert, F. Koch, H. Maier, *Scripta Materialia* 61 (2009) 789
- [11] M.P. Singh, T. Shripathi, K. Shalini, S.A. Shivashankar, *Materials Chemistry and Physics* 105 (2007) 433.
- [12] G. Scarel, A. Svane, M. Fanciulli, *Topics in Applied Physics* 106 (2007) 1.
- [13] G.C. Deepak, N. Bhat, *ECS Transactions* 19 (2009) 175.
- [14] V. Mikhelashvili, G. Eisenstein, F. Edelmann, *J. Appl. Phys.* 90 (2001) 5447.
- [15] M.P. Singh, C.S. Thakur, K. Shalini, N. Bhat, S.A. Shivashankar, *Appl. Phys. Lett.* 83 (2003)

2889.

- [16] M. Losurdo, M.M. Giangregorio, P. Capezzuto, G. Bruno, G. Malandrino, I.L. Fragala, L. Armelao, D. Barreca, E. Tondello, J. Electrochem. Soc. 155 (2008) G44.
- [17] J. Paivasaari, M. Putkonen, T. Sajavaara, L. Niinisto, J. Alloys Compd. 374 (2004) 124.
- [18] J. Paivasaari, J. Niinisto, K. Arstila, K. Kukli, M. Putkonen, L. Niinisto, Chem. Vap. Deposition 11 (2005) 415.
- [19] J. Niinisto, M. Putkonen, L. Niinisto, K. Kukli, M. Ritala, M. Leskela, J. Appl. Phys. 95 (2004) 84.
- [20] J. Niinisto, M. Putkonen, L. Niinisto, K. Arstila, T. Sajavaara, J. Lu, K. Kukli, M. Ritala, M. Leskela, J. Electrochem. Soc. 153 (2006) F39.
- [21] P. Majumder, G. Jursich, A. Kuelto, C. Takoudis, J. Electrochem. Soc. 155 (2008) G152.
- [22] M. Nolan, S.D. Elliott, Chem. Mater. 22 (2010) 117.
- [23] T.V. Trinh, J.P. Chang, Appl. Surf. Sci. 246 (2005) 250.
- [24] Inorganics and related compounds, Sadtler Research Laboratories, Inc. , 1967.
- [25] NIST X-ray Photoelectron Spectroscopy Database Version 3.2 (2007).
- [26] L. Armelao, D. Barreca, G. Bottaro, A. Gasparotto, D. Leonarduzzi, C. Maragno, E. Tondello, Surface Science Spectra 11 (2004) 26.
- [27] M.F. Al-Kuhaili, S.M.A. Durrani, Thin Solid Films 515 (2007) 2885.
- [28] S. Scalese, S. Mirabella, A. Terrasi, Appl. Surf. Sci. 220 (2003) 231.

### Figure Captions

- Figure 1. Schematic diagram of the ALD system used for the deposition of erbium oxide films on Si substrates from tris(methylcyclopentadienyl)erbium and ozone.
- Figure 2.  $\text{Er}_2\text{O}_3$  ALD rate as a function of reactor temperature. The vertical error bars indicate film uniformity across the sample. The bubbler temperature was 95 °C. The system pressure was 0.5 torr.
- Figure 3. Number of cycles vs  $\text{Er}_2\text{O}_3$  film thickness. Linear film growth with increasing number of ALD cycles is observed. The films were deposited at 250 °C and 0.5 torr.
- Figure 4. Transmission absorption FTIR spectra collected at 90 ° take-off angle to the normal of as-deposited  $\text{Er}_2\text{O}_3$  and post-deposition annealed films at the indicated temperature for 5 min in  $\text{N}_2$ . The spectra shown are obtained after subtraction of background spectra obtained from cleaned Si substrate prior to deposition. The films were deposited on p-type Si (100) substrate at a substrate temperature of 250 °C and chamber pressure of 0.5 torr.
- Figure 5. Core level Er 4d, Si 2p and O 1s XPS spectra of as-deposited  $\text{Er}_2\text{O}_3$  film (2 nm-thick) collected at 90 ° take-off angle. Er 4d and Si 2p XP spectra of as-deposited  $\text{Er}_2\text{O}_3$  film (a) and O 1s features of as-deposited film (b). All ALD conditions are the same as those in Fig. 4.

Figure 6. C 1s XP spectra of as-deposited  $\text{Er}_2\text{O}_3$  films (30 nm-thick) collected at  $90^\circ$  take-off angle before and after sputtering using  $\sim 300$  nA beam current argon ion gun for 10 min. Deposition conditions are the same as those in Fig. 4.

Figure 7. Er 4d core level (a) and O 1s XP (b) spectra of as-deposited  $\text{Er}_2\text{O}_3$  (3 nm-thick) collected at  $90^\circ$  take-off angle. The spectra are collected before and after post-deposition annealing in  $\text{N}_2$  for 5 min at the temperature shown. All ALD conditions are the same with those in Fig. 4.

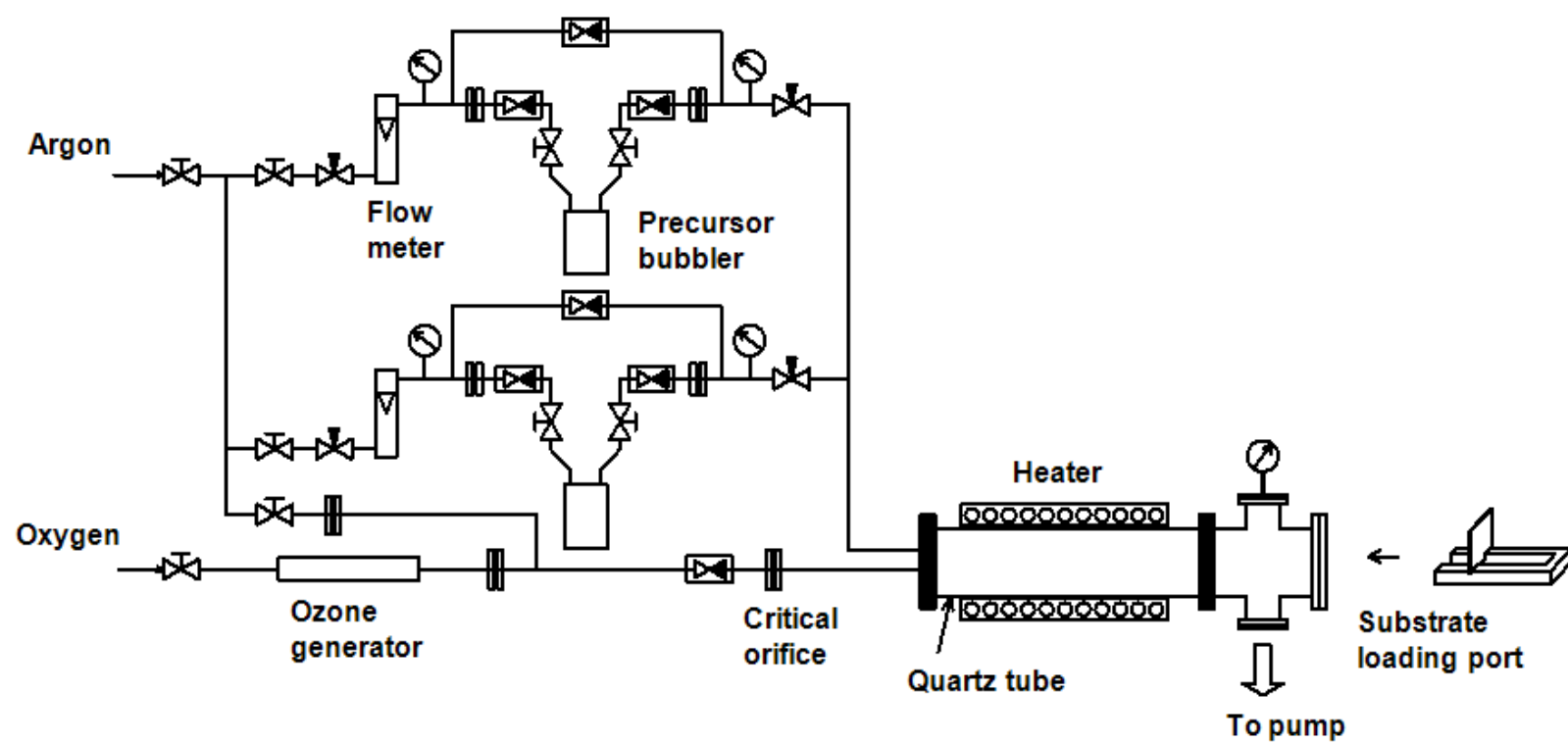
Figure 8. GIXRD of as-deposited and annealed  $\text{Er}_2\text{O}_3$  films (30 nm-thick) at 600, 800 and 1000  $^\circ\text{C}$  in  $\text{N}_2$  at 1 atm, for 5 min. The GIXRD analyses were carried out at a glancing angle of  $0.7^\circ$ . Deposition conditions are the same as those in Fig. 4.

Figure 9. PSI images of  $\text{Er}_2\text{O}_3$  30 nm-thick as-deposited films (a), and films annealed at 600  $^\circ\text{C}$  (b), 800  $^\circ\text{C}$  (c) and 1000  $^\circ\text{C}$  (d) in  $\text{N}_2$  at 1 atm. Film RMS roughness values are 0.71 (a), 0.75 (b), 0.85 (c) and 0.91 nm (d), respectively. Image size:  $229.3 \times 301.5 \mu\text{m}$ . Other film growth conditions are the same as those in Fig. 4.



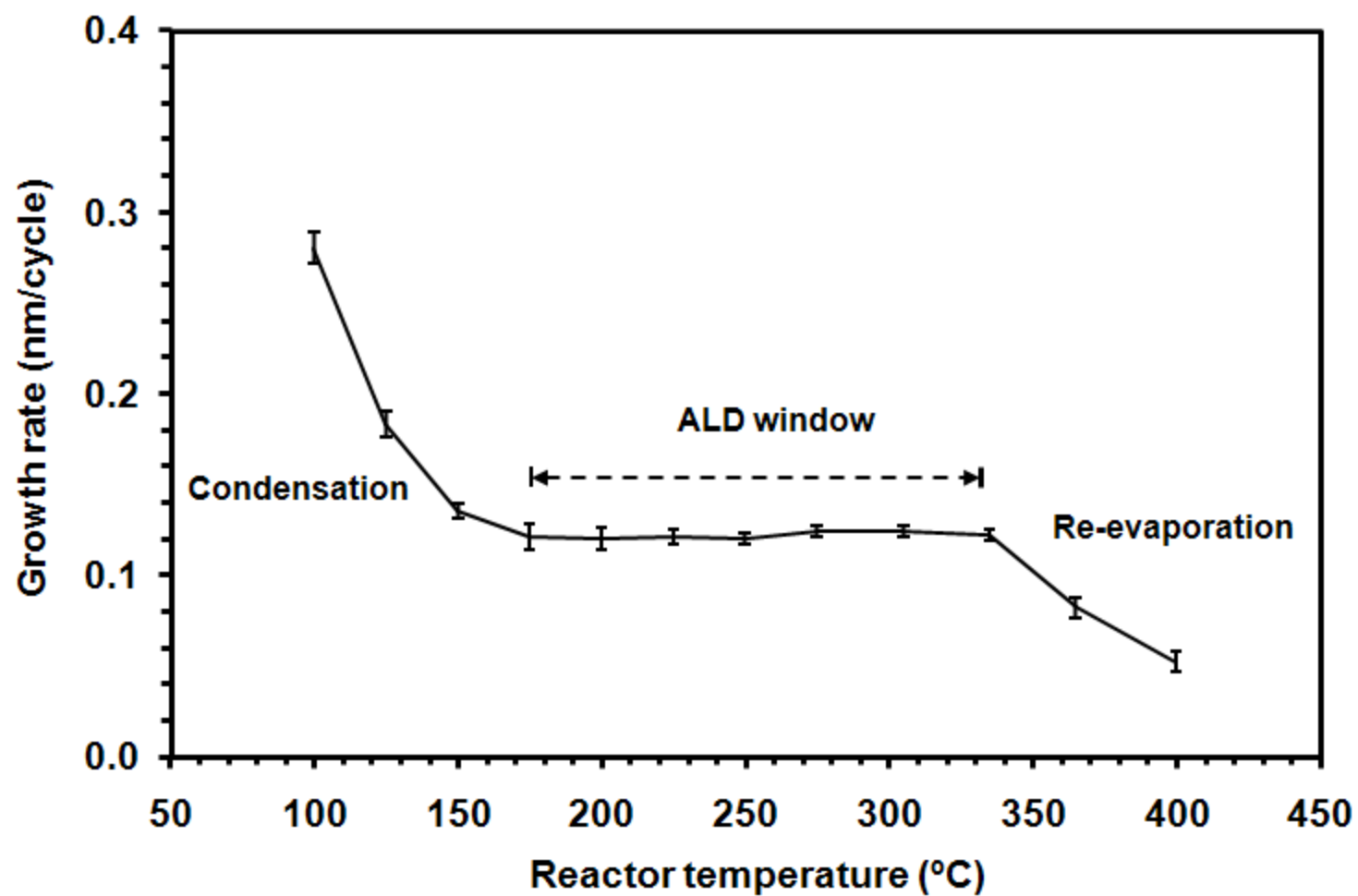
Figure(1)

[Click here to download Figure\(s\): Figure1.ppt](#)



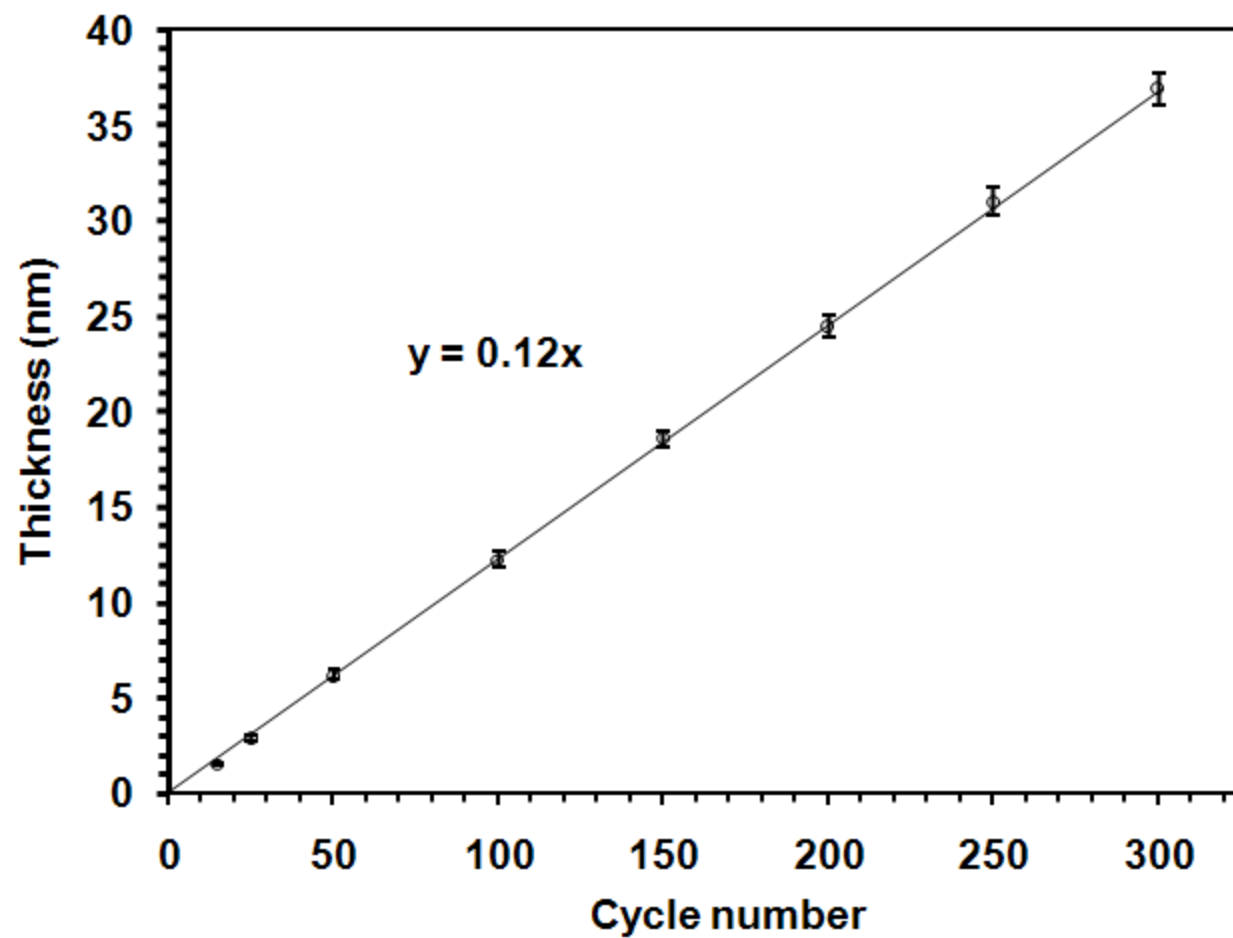
Figure(2)

[Click here to download Figure\(s\): Figure2.ppt](#)



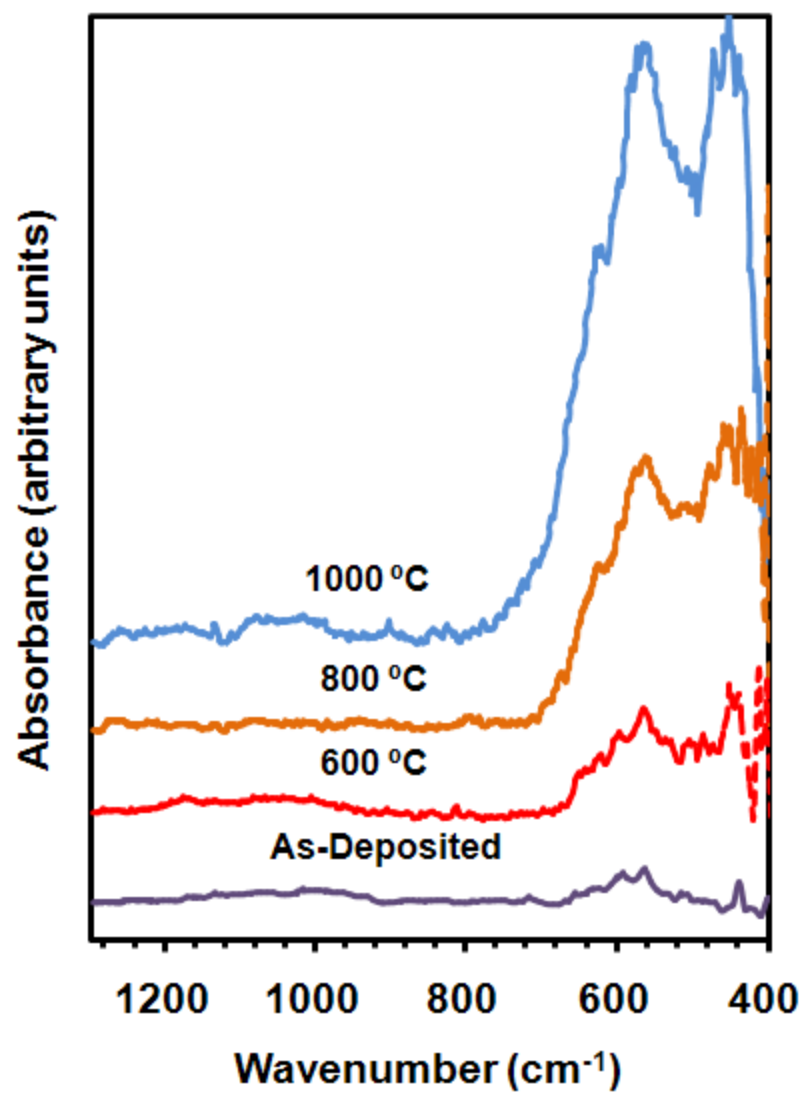
Figure(3)

[Click here to download Figure\(s\): Figure3.ppt](#)



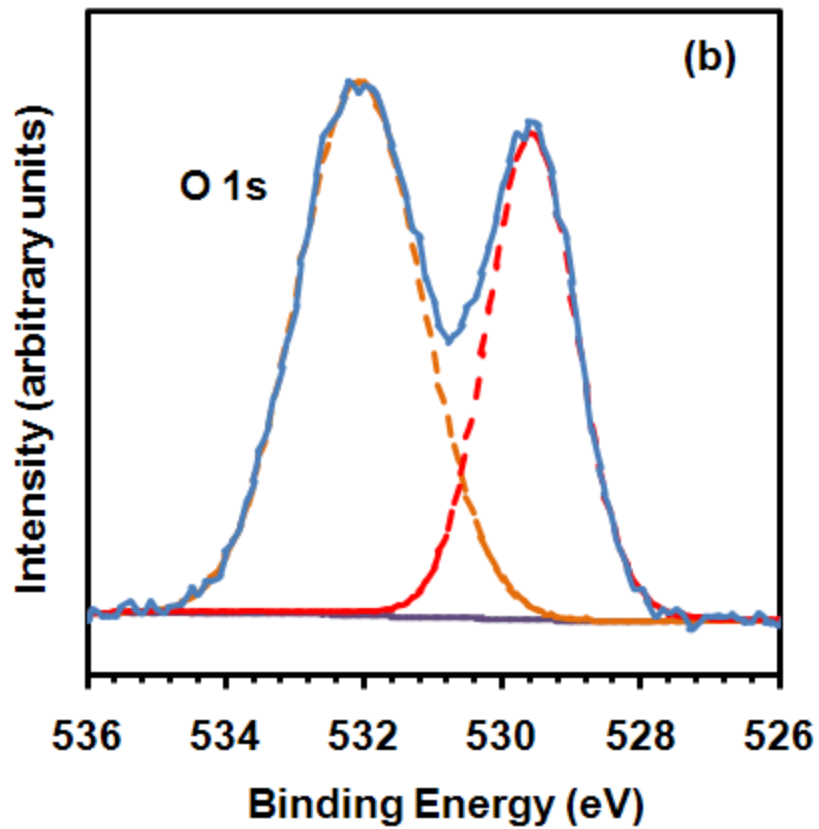
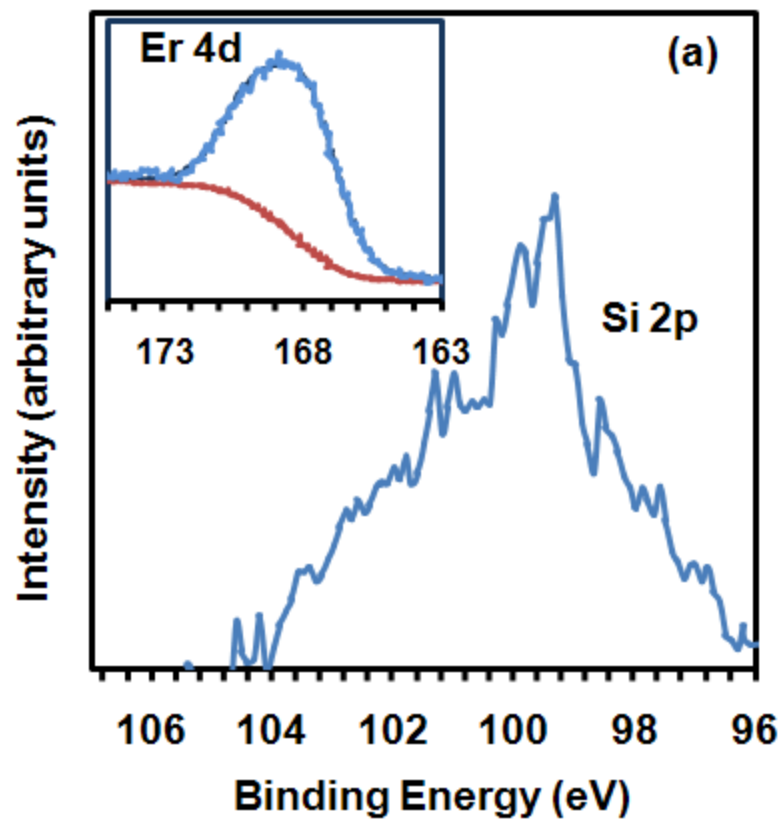
Figure(4)

[Click here to download Figure\(s\): Figure4.ppt](#)



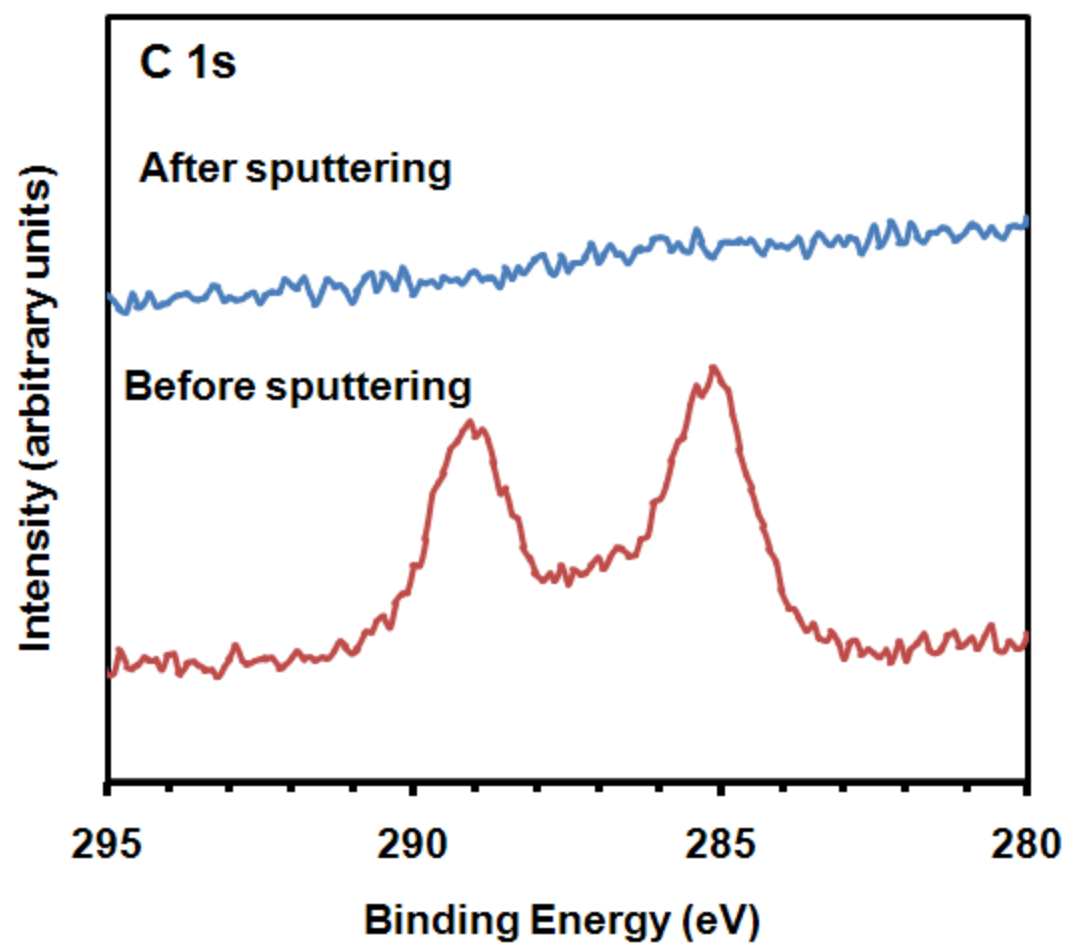
Figure(5)

[Click here to download Figure\(s\): Figure5.ppt](#)

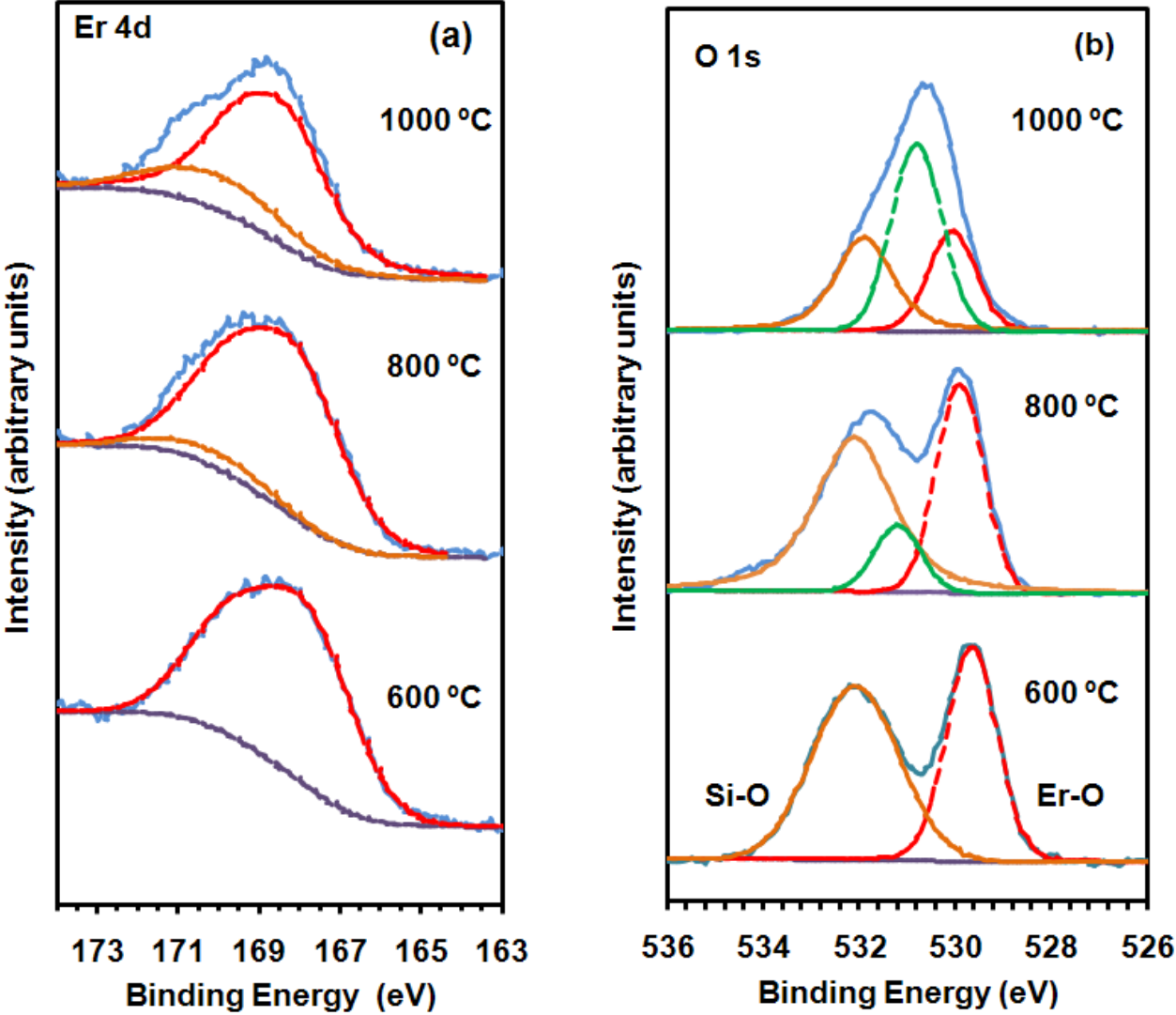


Figure(6)

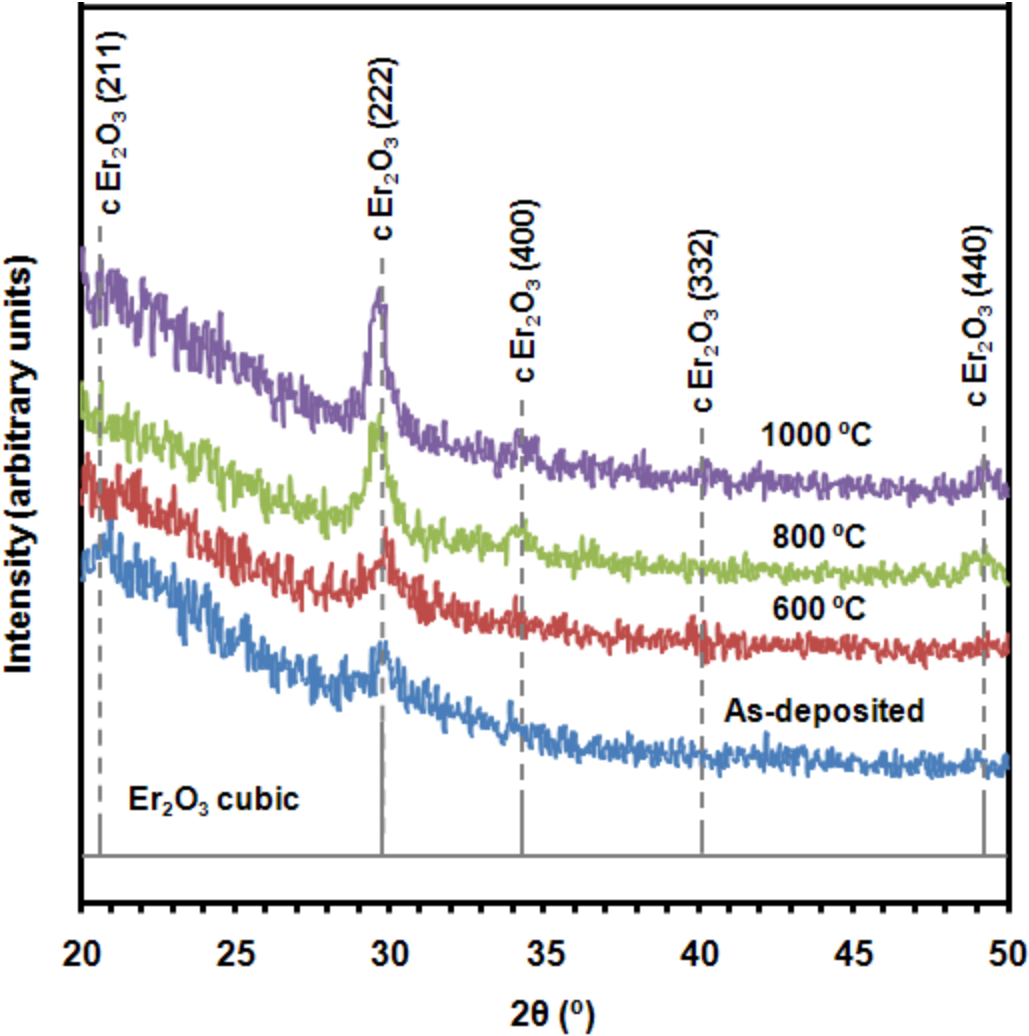
[Click here to download Figure\(s\): Figure6.ppt](#)



Figure(7)  
[Click here to download Figure\(s\): Figure7.ppt](#)



Figure(8)  
[Click here to download Figure\(s\): Figure8.ppt](#)





**Figure(9)**  
[Click here to download Figure\(s\): Figure9.ppt](#)

